



Trade Science Inc.

# Nano Science and Nano Technology

*An Indian Journal*

*Full Paper*

NSNTAJ, 4(1), 2010 [36-41]

## Investigation of thermal resistance of the giant magneto-resistance samples by the PTD technique

T.Ghrib<sup>1\*</sup>, M.S.Ben Kraiem<sup>2</sup>, C.Bordel<sup>3</sup>, N.Yacoubi<sup>1</sup>, A.Cheikhrouhou<sup>2</sup>

<sup>1</sup>Photothermal Laboratory, IPEIN, 8000 Nabeul, (TUNISIA)

<sup>2</sup>Laboratoire de Physique des Materiaux, Faculte des Sciences de Sfax, B.P. 802-3018 Sfax, (TUNISIE)

<sup>3</sup>Groupe de Physique des Matériaux UNR CNRS 6634, BP12, Saint etienne du Rouvay Cedex, (FRANCE)

E-mail : taheer.ghrib@yahoo.fr

Received: 10<sup>th</sup> March, 2010 ; Accepted: 20<sup>th</sup> March, 2010

### ABSTRACT

Investigation of thermal properties giant magneto-resistance constituted with an assembly of alternated Mn/Fe layers according to the Mn thickness using the Photothermal Deflexion Technique. We show in this work that the thermal resistance passes by a maximum value for a Mn critical thickness corresponding to the antiparallel ferromagnetic coupling.

© 2010 Trade Science Inc. - INDIA

### KEYWORDS

Giant magneto-resistance;  
Thermal resistance;  
Photothermal deflexion  
technique.

### INTRODUCTION

Since the years 1980 many research were carried out on the multi-layers magnetic containing ferromagnetic and nonmagnetic materials. Indeed, in 1988 Albert Fert<sup>[1]</sup> and Peter Grünberg<sup>[2,3]</sup> have invented Giant magneto-resistance (GMR) in crystalline mono layers what enables them to receive the Physics Nobel Prize in October 2007.

The GMR samples are an assembly of multi-layers alternated by ferromagnetic-metal and nonmagnetic-metal (FM/NM) with thicknesses of about 1nm.

One of the first manifestations of the new properties of these structures was the observation, in 1986, of an antiferromagnetic coupling between layers of iron in three layers Fe/Cr/Fe deposited by epitaxially molecular jets on AsGa<sup>[2]</sup>.

Several theorists such as Camley, Trigui, Barthélémy<sup>[4-7]</sup> and all tried to develop mathematical models allowing the interpretation of these multi-layers. Duvail and Al<sup>[7-9]</sup> were interested in the dependence

versus the temperature and thickness to the resistivity and the magneto-resistance of multi-layer Co/Cu.

During these 30 years ago the very fundamental interest of the GMR samples is due to its very specific magnetic properties, which are briefly described as follow, the ferromagnetic-metal is microscopically formed of small zones called Weiss-zones. Each zone is characterized by magnetic moments directed in the same direction. In the case of a small lateral dimensions a magnetic interaction between the ferromagnetic layer giving a global magnetizations oriented in the same direction, one says for this balance situation that there is a parallel coupling between the magnetic-layers. By increasing thins of the nonmagnetic-metal layers, one cross a value which beyond the coupling becomes antiparallel.

The resistance is higher for antiparallel configuration and smaller for parallel magnetization configuration.

In this work we study the effect of the Mn layers thickness variations on the thermal properties of the GMR samples constituted on an assembly of alternated

thin layers respectively to Manganese Mn (nonmagnetic metal) of variable thickness from 0.3 to 1.7  $\mu\text{m}$  and to iron Fe (metal ferromagnetic) thickness equalizes to 1.5  $\mu\text{m}$ .

The thermal properties are determined by the Photo-Thermal Deflection (PTD) technique<sup>[8-10]</sup> which will be developed later.

### Sample preparation

The evaporation enclosure is equipped with a turbomolecular pump, which will be aspirated during one week at a temperature of 150°C, which gives a vacuum of about 10<sup>-9</sup> mbar. The materials to evaporate Mn and Fe are placed in alumina crucibles and are heated by radiation until a temperature of 1250°C. Each cell of overflowing has a mask with electro-pneumatic order, which makes it possible to deposit alternatively the various materials without stopping their evaporations.

These layers are deposited with deposit rates of  $2.10^{-12}\text{m.s}^{-1}$  for iron and  $6.10^{-12}\text{m.s}^{-1}$  for manganese. The thickness of each deposited layer is given only after the deposit end, thanks to a quartz oscillator calibrated at the deposition temperature. We obtain an assembling composed of 21 layers deposited on silicon substrate respectively placed as follow: Si, Mn, Fe, Mn, . . . . Fe, Mn.

The last layer of Mn is a protective coating of constant depth equal to 22nm and also the thickness of iron layers are all equal to 1.5nm. For each sample one takes the same thickness for all the layers. This thickness varies from a sample to another from 0.3nm to 1.7nm.

### Magnetic properties

The investigation of the Magnetizations versus the magnetization gives Hysteresis cycles whose form indicates that the iron layers, in the obtained multi-layers are coupled antiparallel for a manganese thickness equal to 1.8nm and coupled parallel for a manganese thickness less than 1.2nm.

It is noticed that, more the value of Mn thickness is large, more the cycles are flat, i.e., more need for applying a large field H to reach the saturation et this is for an antiparallel coupling. Whereas for a thin Mn layers the form of the Hysteresis cycles are identical and show that the obtaining of the saturation magnetization is for

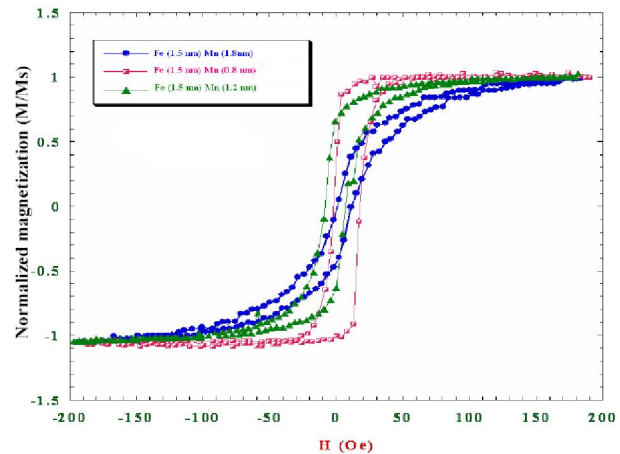


Figure 1 : Representation M-H loops for Fe-Mn GMR samples for 0.8, 1.2 and 1.8nm thickness of the Mn layer

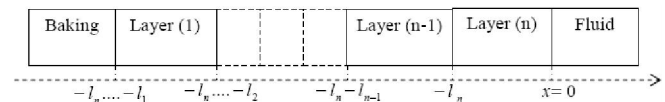


Figure 2 : Different medias browsed by the heat

low values of the applied field H.

The thermal properties are determined with the Photo-Thermal Deflection (PTD) technique.

### Thermal properties

The thermal properties such as the thermal conductivity and the thermal properties are determined by the PTD technique.

### Principle of the PTD technique

This method consists in heating a sample with a modulated light beam of intensity  $I = I_0(1 + \cos\omega t)$ . The thermal wave generated by the optical absorption of the sample will propagate in the sample and in the surrounding fluid (air in our case). The thermal wave in the fluid will induce a temperature gradient then a refractive index gradient in the fluid which will cause the deflection  $\psi$  of a probe Laser beam skimming the sample surface. This deflection may be related to the thermal properties of the sample.

The sample is a stack of 21 layers, we write the heat equations in these areas and in the two surrounding fluid which are the air in by designating  $K_1$ ,  $D_1$  and  $l_1$  respectively the thermal conductivity, the thermal Diffusivity and the thickness of the layer  $i$ .

### Theoretical model

#### Probe beam deflection

In the case of a uniform heating we can use a 1-

## Full Paper

dimensional approximation, and the amplitude  $|\psi|$  and phase  $\varphi$  of the probe beam deflection  $\psi$  is given by:

$$|\psi| = \frac{\sqrt{2} L}{n \mu_f} \frac{dn}{dT_f} |T_0| e^{-\frac{x}{\mu_f}} \quad \text{and} \quad \varphi = -\frac{x}{\mu_f} + \theta + \frac{5\pi}{4}$$

where  $l$  is the width of the pump beam in the direction of the probe laser beam,  $n$ ,  $\mu_f$  and  $T_f$  are respectively the refractive index, the thermal diffusion length and the temperature of the fluid.  $|T_0|$  and  $\theta$  are respectively the amplitude and phase of the temperature  $T_0$  at the sample surface which are function of the thermal properties of the different media.  $x$  is the distance between the probe beam axe and the sample surface.

Before the calculation of the probe beam deflection, one must know the expression of the surface temperature  $T_0$  that is calculated follow.

### Surface temperature

The resolution of the heat equation gives the following temperature equation:

$$T_f(x,t) = T_0 e^{-\sigma_f x} e^{j\omega t}$$

if  $0 \leq x \leq l_f$

$$T_n(x,t) = (X_n e^{\sigma_n x} + Y_n e^{-\sigma_n x} - E_n e^{\alpha_n x}) e^{j\omega t}$$

if  $-l_n \leq x \leq 0$

$$T_{n-1}(x,t) = (X_{n-1} e^{\sigma_{n-1}(x+l_n)} + Y_{n-1} e^{-\sigma_{n-1}(x+l_n)} - E_{n-1} e^{\alpha_{n-1}(x+l_n)}) e^{j\omega t}$$

if  $-l_n - l_{n-1} \leq x \leq -l_{n-1}$

$$T_1(x,t) = (X_1 e^{\sigma_1(x+l_n+l_{n-1}+\dots+l_2)} + Y_1 e^{-\sigma_1(x+l_n+l_{n-1}+\dots+l_2)} - E_1 e^{\alpha_1(x+l_n+l_{n-1}+\dots+l_2)}) e^{j\omega t}$$

if  $-l_n - l_{n-1} - \dots - l_1 \leq x \leq -l_n - l_{n-1} - \dots - l_2$

$$T_b(x,t) = W e^{\sigma_b(x+l_n+l_{n-1}+\dots+l_2+l_1)} e^{j\omega t}$$

if  $-l_n - l_{n-1} - \dots - l_1 - l_b \leq x \leq -l_n - l_{n-1} - \dots - l_1$

And after, we write the flow equation in each medium

$$\phi_f(x,t) = K_f \sigma_f T_0 e^{-\sigma_f x} e^{j\omega t}$$

if  $0 \leq x \leq l_f$

$$\phi_n(x,t) = -K_n \sigma_n (X_n e^{\sigma_n x} - Y_n e^{-\sigma_n x} - \frac{\alpha_n}{\sigma_n} E_n e^{\alpha_n x}) e^{j\omega t}$$

if  $-l_n \leq x \leq 0$

$$\phi_{n-1}(x,t) = -K_{n-1} \sigma_{n-1} (X_{n-1} e^{\sigma_{n-1}(x+l_n)} -$$

$$Y_{n-1} e^{-\sigma_{n-1}(x+l_n)} - \frac{\alpha_{n-1}}{\sigma_{n-1}} E_{n-1} e^{\alpha_{n-1}(x+l_n)}) e^{j\omega t}$$

if  $-l_n - l_{n-1} \leq x \leq -l_{n-1}$

$$\phi_1(x,t) = -K_1 \sigma_1 (X_1 e^{\sigma_1(x+l_n+l_{n-1}+\dots+l_2)} -$$

$$Y_1 e^{-\sigma_1(x+l_n+l_{n-1}+\dots+l_2)} - \frac{\alpha_1}{\sigma_1} E_1 e^{\alpha_1(x+l_n+l_{n-1}+\dots+l_2)}) e^{j\omega t}$$

if  $-l_n - l_{n-1} - \dots - l_1 \leq x \leq -l_n - l_{n-1} - \dots - l_2$

$$\phi_b(x,t) = -K_b \sigma_b W e^{\sigma_b(x+l_n+l_{n-1}+\dots+l_2+l_1)} e^{j\omega t}$$

if  $-l_n - l_{n-1} - \dots - l_1 - l_b \leq x \leq -l_n - l_{n-1} - \dots - l_1$

The temperature and heat flow continuity at the interface  $x = -l_n$  permit to obtain:

$$\begin{pmatrix} 1 & 1 & -1 \\ 1 & -1 & -r_{n-1} \\ 0 & 0 & E_n/E_{n-1} \end{pmatrix} \begin{pmatrix} X_{n-1} \\ Y_{n-1} \\ E_{n-1} \end{pmatrix} =$$

$$\begin{pmatrix} e^{-\sigma_n l_n} & e^{\sigma_n l_n} & -e^{-\alpha_n l_n} \\ c_n e^{-\sigma_n l_n} & -c_n e^{\sigma_n l_n} & -c_n r_n e^{-\alpha_n l_n} \\ 0 & 0 & 1 \end{pmatrix} \begin{pmatrix} X_n \\ Y_n \\ E_n \end{pmatrix}$$

$$G_n \begin{pmatrix} X_{n-1} \\ Y_{n-1} \\ E_{n-1} \end{pmatrix} = D_n \begin{pmatrix} X_n \\ Y_n \\ E_n \end{pmatrix} \quad \text{Or}$$

$$\begin{pmatrix} X_{n-1} \\ Y_{n-1} \\ E_{n-1} \end{pmatrix} = G_n^{-1} \cdot D_n \begin{pmatrix} X_n \\ Y_n \\ E_n \end{pmatrix} = M_n \begin{pmatrix} X_n \\ Y_n \\ E_n \end{pmatrix}$$

$$\text{Where, } G_n = \begin{pmatrix} 1 & 1 & -1 \\ 1 & -1 & -r_{n-1} \\ 0 & 0 & E_n/E_{n-1} \end{pmatrix},$$

$$D_n = \begin{pmatrix} e^{-\sigma_n l_n} & e^{\sigma_n l_n} & -e^{-\alpha_n l_n} \\ c_n e^{-\sigma_n l_n} & -c_n e^{\sigma_n l_n} & -c_n r_n e^{-\alpha_n l_n} \\ 0 & 0 & 1 \end{pmatrix},$$

and  $M_n = G_n^{-1} \cdot D_n$

In the same way we can write in the interface  $x_i = -$

$$l_n - l_{n-1} - \dots - l_i \begin{pmatrix} X_{i-1} \\ Y_{i-1} \\ E_{i-1} \end{pmatrix} = M_i \begin{pmatrix} X_i \\ Y_i \\ E_i \end{pmatrix}$$

Then,

$$\begin{pmatrix} X_1 \\ Y_1 \\ E_1 \end{pmatrix} = M_2 \cdot M_3 \cdot \dots \cdot M_n \begin{pmatrix} X_n \\ Y_n \\ E_n \end{pmatrix} = \begin{pmatrix} m_{11} & m_{12} & m_{13} \\ m_{21} & m_{22} & m_{23} \\ m_{31} & m_{32} & m_{33} \end{pmatrix} \begin{pmatrix} X_n \\ Y_n \\ E_n \end{pmatrix}$$

In this case we write

$$\begin{cases} X_1 = m_{11} X_n + m_{12} Y_n + m_{13} E_n \\ Y_1 = m_{21} X_n + m_{22} Y_n + m_{23} E_n \end{cases}$$

The writing of the heat flow and temperature continuity at the interfaces  $x = 0$  and  $x = -l_3 - l_2 - l_1$  give respectively:

$$X_n = \frac{1}{2}(1-g)T_0 + (1+r_3)\frac{E_n}{2}, \quad Y_n = \frac{1}{2}(1+g)T_0 + (1-r_3)\frac{E_n}{2}$$

And

$$(1-b)e^{-\sigma_1 t_1} X_1 - (1+b)e^{\sigma_1 t_1} Y_1 - (r_1-b)e^{-\alpha_1 t_1} E_1 = 0 \quad (1)$$

$$X_1 = \frac{m_{11}}{2}((1-g)T_0 + (1+r_n)E_n) +$$

Then 
$$\frac{m_{12}}{2}((1+g)T_0 + (1-r_n)E_n) + m_{13}E_n$$

$$Y_1 = \frac{m_{21}}{2}((1-g)T_0 + (1+r_n)E_n) +$$

and 
$$\frac{m_{22}}{2}((1+g)T_0 + (1-r_n)E_n) + m_{23}E_n$$

$$X_1 = (m_{11}(1-g) + m_{12}(1+g))\frac{T_0}{2} +$$

Or too 
$$(m_{11}(1+r_n) + m_{12}(1-r_n) + 2m_{13})\frac{E_n}{2}$$

$$Y_1 = (m_{21}(1-g) + m_{22}(1+g))\frac{T_0}{2} +$$

and 
$$(m_{21}(1+r_n) + m_{22}(1-r_n) + 2m_{23})\frac{E_n}{2}$$

That is to say  $X_1 = \eta_1 T_0 + \eta_2 E_n$  and  $Y_1 = \eta_3 T_0 + \eta_4 E_n$

By replacing  $X_1$  and  $Y_1$  by its expressions in equation (1) one obtains:

$$(1-b)e^{-\sigma_1 t_1} (\eta_1 T_0 + \eta_2 E_n) - (1+b)e^{\sigma_1 t_1} (\eta_3 T_0 + \eta_4 E_n) - (r_1-b)e^{-\alpha_1 t_1} E_1 = 0$$

What gives

$$((1-b)\eta_1 e^{-\sigma_1 t_1} - (1+b)\eta_3 e^{\sigma_1 t_1}) T_0 = ((1+b)\eta_4 e^{\sigma_1 t_1} - (1-b)\eta_2 e^{-\sigma_1 t_1}) E_n + (r_1-b)e^{-\alpha_1 t_1} E_1$$

Finally

$$T_0 = \frac{[(1+b)\eta_4 e^{\sigma_1 t_1} - (1-b)\eta_2 e^{-\sigma_1 t_1}] E_n + (r_1-b)e^{-\alpha_1 t_1} E_1}{[(1-b)\eta_1 e^{-\sigma_1 t_1} - (1+b)\eta_3 e^{\sigma_1 t_1}]}$$

With 
$$E_i = \frac{\alpha_i}{2K_{ci}(\alpha_i^2 - \sigma_i^2)}$$

### Experimental set-up

The sample is heated by a halogen lamp light of Power 100W modulated thanks a mechanical chopper at a variable frequency. A (He-Ne) Laser probe beam skimming the sample surface at a distance  $z$  is deflected. This deflection can be detected by a four quadrant

photo-detector and converted to an electrical signal which is measured by a lock-in amplifier. Through the intermediary of interfaces, the mechanical chopper and the Look-in amplifier a microcomputer will set the desired modulation frequency and read the values of the amplitude and phase of the photo-thermal signal and then draw their variations according to the square root modulation frequency.

### Determination of the thermal properties

In order to determine the thermal properties of the seven samples we have plotted on figure 4 the experimental variation of phase and normalized amplitude of the PTD signal versus the square root modulation frequency. The difference between these curves is attributed to the difference of their thermal conductivity, thermal diffusivity and absorption coefficient. Using the theoretical model presented in section 2 one can deduce this thermal properties ( $K_i$ ,  $D_i$ ) and optical absorption  $\alpha_i$ .

The TABLE 1 gives the thermal conductivities, the thermal diffusivities and the absorption coefficients of

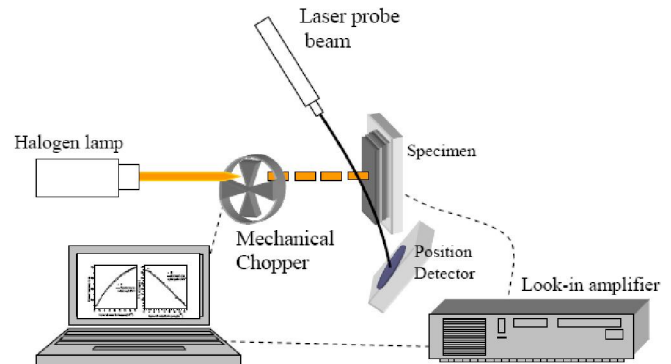
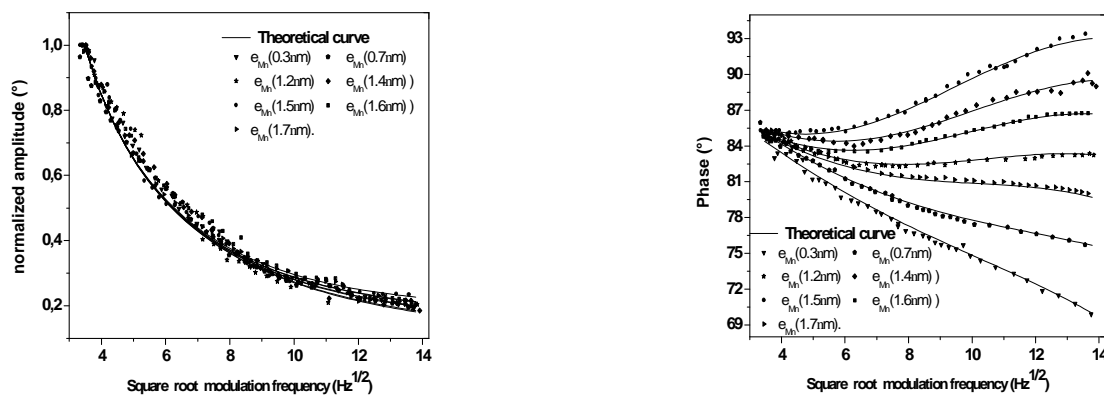


Figure 3 : Schematic experimental setup

TABLE 1 : Evolution of the thermal conductivities, thermal diffusivities and absorption coefficient of the Fe and Mn layer in the GMR samples for various Mn thickness

Thickness (nm)	Thermal conductivity ( $W.m^{-1}.K^{-1}$ )		Thermal diffusivity ( $10^{-4} m^2.s^{-1}$ )		Absorption coefficient ( $m^{-1}$ )		
	Fe	Mn	Fe	Mn	Fe	Mn	
1.5	0.3	0.36	0.05	0.22	0.01	$10^{-3}$	$2 \times 10^5$
1.5	0.7	0.34	0.032	0.22	0.01	$10^{-3}$	$2.7 \times 10^6$
1.5	1.2	0.31	0.013	0.22	0.01	$10^{-3}$	$3.3 \times 10^6$
1.5	1.4	0.19	0.0076	0.22	0.01	$10^{-3}$	$4.7 \times 10^6$
1.5	1.5	0.084	0.0064	0.22	0.01	$10^{-3}$	$6.1 \times 10^6$
1.5	1.6	0.32	0.0092	0.22	0.01	$10^{-3}$	$3.6 \times 10^6$
1.5	1.7	1.13	0.03	0.22	0.01	$10^{-3}$	$3 \times 10^6$

## Full Paper



**Figure 4 :** Normalized amplitude and phase of the photothermal signal versus the square root modulation frequency for different Mn thickness

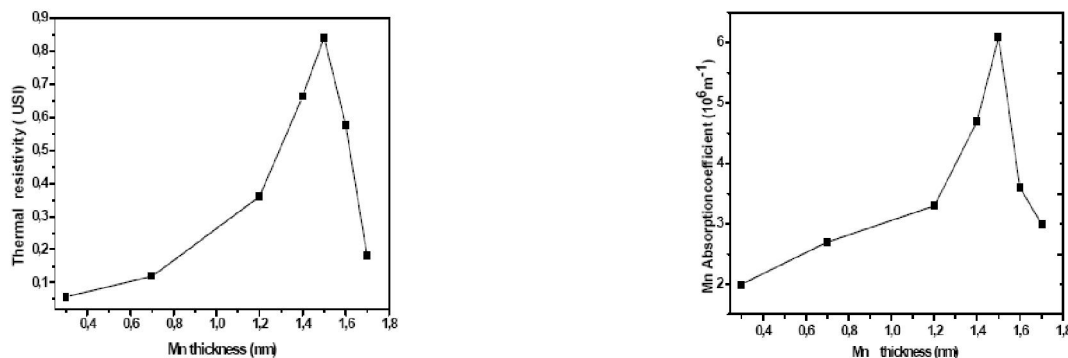


**Figure 5 :** Thermal resistivity and Mn absorption coefficient of the GMR samples evolution with the Mn thickness

the Mn and Fe layers in the GMR samples for all manganese thicknesses. We notice that only thermal conductivities of the materials kinds and the Mn absorption coefficient vary by increasing the Mn thickness.

We can see from this table that only the thermal conductivities of both layers and the absorption coefficient of Mn layers vary by varying the thickness of the Mn layer.

The thermal resistance of the sample is given by

$$R_{th} = \frac{1}{S} \sum_i \frac{e_i}{K_i}$$

Where  $e_i$ ,  $S$  and  $K_i$  are respectively the thickness, the surface and the thermal conductivity of the sample and for a surface equal to  $S = 1\text{cm}^2$  we can trace the evolution of the thermal resistance of the GMR materials versus the Mn thickness as shown in figure 4. We notice from these curves that the thermal resistance and the Mn absorption coefficient are maximum for a Mn thickness equal to 1.5nm. According to study proposed in section IV this thickness correspond to transition ferromagnetic parallel-antiparallel and more precisely corresponds to an antiparallel coupling of the dipoles. Several experimental studies<sup>[1-3,7,9]</sup> showed that

the magneto-resistance passes also by a maximum value for a critical thickness of nonmagnetic material. Then one can deduce a mathematical relation which relates the magnetic and thermal resistances like that proposed by Wiedemann-Franz<sup>[10]</sup>  $K_c = \sigma LT$  giving a relationship between the electronic conductivity of the heat  $K_c$  to the electric conductivity  $\sigma$ , where  $L = 2.4 \times 10^{-8}\text{USI}$  and  $T$  is the sample temperature, witch shows that the two parameters have the same evolution.

## CONCLUSION

In this work we have studied the evolution of the thermal properties of the giant magneto-resistance sample constituted with an assembly of alternated Mn/Fe layers with photothermal deflection technique by clarifying the mathematical model which accompanies it. And after the determination of the Mn and Fe thermal conductivities we have determined the thermal resistance evolution via Mn thickness, we noticed that it passes by a maximum value for a Mn critical thickness corresponding to an antiparallel ferromagnetic coupling.

**REFERENCES**

- [1] M.N.Baibich, J.M.Broto, A.Fert, F.Nguyen Van Dau, F.Petroff, P.Etienne, G.Creuzet, A.Friederich, J.Chazelas; *Phys.Rev.Lett.*, **61**, 2472 (1988).
- [2] P.Grünberg, R.Schreiber, Y.Pang, M.B.Brodsky, H.Sowers; *Phys.Rev.Lett.*, **57**, 2442 (1986).
- [3] G.Binash, P.Grünberg, F.Saurenbach, W.Zinn; *Phys.Rev.B*, **39**, 4828 (1989).
- [4] R.E.Camley, J.Barnas; *Phys.Rev.Lett.*, **63**, 664 (1989).
- [5] F.Trigui, E.Velu, C.Dupas; *J.Magn.Magn.Mater.*, **93**, 421 (1991).
- [6] A.Barthélémy, A.Fert; *Phys.Rev.B*, **43(13)**, 124 (1991).
- [7] Zhao Pingbo, Li Bozang, Pu Fuke; *Chin.Phys.Lett.*, **12(8)**, 485 (1995).
- [8] J.L.Duvail, A.Fert, L.G.Pereira, D.K.Lottis; *J.Appl. Phys.*, **75**, 7070 (1994).
- [9] S.N.Ohno, K.Inomate; *Phys.Rev.Lett.*, **72**, 1553 (1994).
- [10] X.J.Liu, Q.J.Huang, S.Y.Zhang, A.H.Luo, C.X.Zhao; *J.Phys.Chem.Solids*, **65**, 1247 (2004).